

Mitogen-activated protein kinase inhibitor PD0325901 enhances radiosensitivity by modulating PD-1/PD-L1 through MEK/ERK pathway in cervical cancer cells

Q. Qin¹, C. Liu², J. Lu¹, J. Wang¹, Z. Li^{1*}

¹Department of Gynaecology and Obstetrics, The Second Clinical Medical College, China Three Gorges University, Yichang 443001, Hubei Province, China

²Tumor Microenvironment and Immunotherapy, Hubei Key Laboratory, China Three Gorges University, Yichang 443002, Hubei Province, China

ABSTRACT

► Original article

*Corresponding author:

Zhiying Li, M.D.,

E-mail: teng.prof@gmail.com

Received: July 2025

Final revised: August 2025

Accepted: August 2025

Int. J. Radiat. Res., April 2026;
24(2): 365-371

DOI: 10.61186/ijrr.24.2.10

Keywords: Cervical cancer, MEK inhibitor, PD0325901, MEK/ERK pathway, PD-1/PD-L1, radiosensitization, apoptosis.

Background: To investigate the mechanism of mitogen-activated protein kinase (MEK) inhibitor PD0325901-mediated MEK/extracellular signal-regulated kinase (ERK1)/2 pathway on programmed death-1(PD-1) and ligand programmed death ligand-1(PD-L1) in cervical cancer (CC) cells. **Materials and Methods:** CC HeLa cells were divided into three groups: control (Group A), PD0325901 (100 nmol/L) (Group B), and Phorbol 12-myristate 13-acetate (PMA) (100 nmol/L PD0325901 + 10 μmol/L PMA) (Group C). The methodology used for simulation radiotherapy includes assessing cell viability at 12h and 24h using 3-(4,5-dimethylthiazol-2-yl)-2,5-diphenyltetrazolium bromide (MTT) assay, apoptosis by Annexin V-FITC/PI method, invasion through Transwell assay, and gene expression by reverse transcription polymerase chain reaction (RT-PCR) and Western blot. PD0325901 was tested as a potential radiosensitizer by modulating PD-1/PD-L1 immune checkpoint expression and affecting the MEK/ERK pathway in simulated post-radiotherapy conditions. **Results:** At 12h and 24h, cell viability in Group B was significantly lower than Group A, with increased apoptosis rates in Group B compared to Group A. Group C showed partial reversal of these effects. MEK/ERK1/2, PD-1, and PD-L1 expression were reduced in Group B, but upregulated in Group C, confirming the impact of PD0325901 on immune checkpoint modulation. **Conclusion:** PD0325901 inhibits the MEK/ERK1/2 pathway, leading to suppression of PD-1/PD-L1 expression and enhanced apoptosis in cervical cancer cells, suggesting a potential role for PD0325901 in enhancing radiosensitivity by modulating immune checkpoint signaling.

INTRODUCTION

Cervical cancer (CC) is a common female malignant tumor with high morbidity and mortality. At present, the treatment of CC mainly includes surgery, radiotherapy, chemotherapy and immunotherapy (1). Among these, radiotherapy remains a cornerstone of treatment for both early-stage and advanced CC, particularly in resource-limited settings. However, therapeutic resistance—especially immune evasion—significantly limits radiotherapy efficacy in many patients (1,2).

Immunotherapy, as a new type of treatment, has become a research hotspot in cancer therapy by activating the patient's own immune system to recognize and kill tumor cells (3,4). Programmed death protein 1 (PD-1) is an important immune checkpoint, which is highly expressed in many tumor cells and inhibits T cell activity by binding to programmed death ligand-1 (PD-L1) and PD-L2, thus promoting tumor immune escape. The PD-1 and its ligand PD-L1 is increased in patients with CC, suggesting that PD-1/PD-L1 pathway plays critical role in the occurrence

and development of CC (5). Notably, recent studies indicate that radiation therapy itself may upregulate PD-L1 expression in tumor cells as a resistance mechanism, further promoting immune escape and tumor persistence. This has been experimentally demonstrated in preclinical tumor models where radiotherapy led to increased PD-L1 expression and immune suppression, which was reversed by PD-L1 blockade (6). These findings support the cancer-immune set point theory, where therapeutic outcomes are determined by the balance between immune activation and suppression (7,8). Therefore, blocking the PD-1/PD-L1 axis has emerged as a promising radiosensitization strategy in cervical cancer. These findings support the cancer-immune set point theory, where therapeutic outcomes are determined by the balance between immune activation and suppression (9).

MEK/ERK1/2 pathway is one of the important pathways of cell signal transduction, which is involved in regulating many biological processes such as cell proliferation, and migration. MEK/ERK1/2 pathway plays critical role in the growth, and

metastasis of CC cells. At the same time, MEK/ERK1/2 pathway is also involved in the regulation of PD-1/PD-L1 activity. PD0325901 is a selective MEK inhibitor, which can effectively inhibit the activity of MEK/ERK1/2 pathway⁽¹⁰⁾. PD0325901 can inhibit the growth and proliferation of cancer cells and promote their apoptosis⁽¹¹⁾.

Importantly, MEK inhibition has been shown to reduce PD-L1 expression and restore immune surveillance in various cancer models. These properties suggest that PD0325901 may act as a radiosensitizing agent by disrupting compensatory immune checkpoint upregulation following radiotherapy⁽¹²⁾. However, its potential role in modulating immune escape mechanisms relevant to radiotherapy in cervical cancer remains underexplored.

Therefore, this study will explore the mechanism of the effect of PD0325901-mediated MEK/ERK1/2 pathway on PD-1 and ligand PD-L1 in CC cells, with the aim of providing mechanistic evidence for its potential use in enhancing cervical cancer radiosensitivity and overcoming immune resistance to radiotherapy. The novelty of this study lies in its investigation of PD0325901 as a potential radiosensitizer specifically for cervical cancer, a tumor type with limited treatment options for radiation resistance. Unlike previous studies, this research focuses on modulating the immune checkpoint pathway PD-1/PD-L1 in combination with MEK inhibition, offering a new approach to improving radiotherapy efficacy and tackling immune-mediated resistance mechanisms.

MATERIALS AND METHODS

Methods

CC HeLa cells were purchased from the cell bank of the Chinese Academy of Sciences and cultured in DMEM medium containing 15% fetal bovine serum at 37 °C and 5% CO₂.

Materials

Reagents and instruments

PD0325901-MEK inhibitor (ThermoFisher Scientific, USA), PD-L1 inhibitor (ThermoFisher Scientific, USA), MTT kit (Roche, Germany), Annexin V-FITC/PI detection kit (Roche, Germany), RT-PCR kit (Roche, Germany), Bcl-2 antibody (ThermoFisher Scientific, USA), Bax antibody (ThermoFisher Scientific, USA), MEK/ERK1/2 antibody (ThermoFisher Scientific, USA), GAPDH antibody (ThermoFisher Scientific, USA), protein electrophoresis buffer (Agilent Technologies, USA), PVDF membrane (Agilent Technologies, USA), protein marker (Bio-Rad, USA), cell culture incubator (ThermoFisher Scientific, USA), laser confocal microscope (Leica, Germany), electrophoresis apparatus (Bio-Rad, USA)

Cell grouping and drug administration

HeLa cells were removed from the frozen tube and thawed in a water bath at 37 °C. The cells were inoculated in a culture flask, added with appropriate culture medium, and cultured in a 5% CO₂ incubator at 37 °C. The cells were divided into three groups: Control group (Group A), PD0325901 group (Group B): treated with PD0325901 at a concentration of 100 nmol/L. This dose was selected based on previous studies showing its efficacy in modulating the MEK/ERK signaling pathway and immune checkpoint expression in tumor models, including radiosensitization settings^(11,13). PMA group (Group C): treated with PD0325901 (100 nmol/L) and phorbol 12-myristate 13-acetate (PMA, 10 μmol/L). PMA served as an activator of the ERK1/2 pathway to simulate radiation-induced stress signaling and pathway reactivation following therapy. Although radiation was not directly applied in this study, the experimental design aimed to mimic molecular features relevant to immune modulation and resistance mechanisms observed after radiotherapy in cervical cancer.

MTT assay

4 × 10³ CC HeLa cells were inoculated into 96-well plates and cultured for 24 hours. According to the above scheme, the patients were divided into groups and given drugs, and there were 3 compound holes in each group. After 48 hours, 10 μL MTT solution was added to each well and incubated for 4 hours, and the supernatant was discarded. 100 μL dimethyl sulfoxide was added to oscillate at a low speed to fully dissolve the crystal. The absorbance value (OD value) of each hole was measured by OD490nm using enzyme labeling instrument. The experiment was repeated three times.

Cell viability measured by MTT assay is presented as a bar graph in Figure2, showing OD490 nm values at 12h and 24h for all groups. Error bars indicate standard deviation.

This assay was used to assess tumor cell viability following MEK inhibition, simulating post-radiotherapy conditions where residual tumor proliferation contributes to treatment resistance.

Annexin V-FITC/PI assay

9 × 10³ HeLa cells were inoculated into 6-well plates and cultured for 24 hours. According to the experimental scheme, the cells were divided into three groups, and each group had three replicate wells. After 48 hours of treatment, the cells were digested with trypsin (without EDTA), washed twice with PBS, and 1 × 10⁵ cells were collected after centrifugation. Binding Buffer was added to the cell suspension, followed by 5 μL of Annexin V-FITC and 5 μL of PI, and the mixture was incubated at room temperature for 15 minutes, away from light. Flow cytometry analysis was performed within 1 hour to detect apoptotic cells.

The apoptotic cells were quantified as the sum of early and late apoptotic populations, as shown in Table 3. Since radiation induces cell death primarily through apoptosis, this assay evaluated whether PD0325901 modulates pro-apoptotic signaling relevant to radiosensitization.

Transwell assay

In the initial stage of the experiment, HeLa cells were planted in Transwell cells and filled with matrix glue for subsequent use. After 24 hours of serum starvation, these cells were transferred to the Transwell chamber and cultured in a serum-free medium containing different concentrations of Agamanine. At the same time, the conventional medium was added to the bottom of the room for culture. After 24 hours of culture, the invasive cells were gently wiped off with a sterile cotton swab, then stained with crystal violet, and the cells were counted with the help of a microscope. Radiotherapy is often limited by metastatic escape; therefore, this invasion assay served to evaluate whether MEK inhibition reduces metastatic potential under conditions mimicking post-radiation stress.

RT-PCR

The cultured cells were lysed according to the instructions of TRIzol kit and total RNA was extracted. cDNA was synthesized by reverse transcription kit and used for PCR amplification. Proper amount of buffer, dNTP, MgCl₂, Taq enzyme, primer and cDNA template were added to the PCR reaction tube, and then the reaction tube was put into the PCR instrument. Set the cycle conditions of PCR reaction, such as pre-denaturation (95 °C, 30s), denaturation (95 °C, 30s), annealing (specific temperature, such as 60 °C, 30s) and extension (72 °C, 30s). It usually takes 35-40 cycles to ensure the full amplification of the target gene. The change of fluorescence signal is monitored in real time in the process of PCR reaction. When the reaction reaches a specific stage, the target gene fragment is amplified and the fluorescence signal reaches detectable level, and the instrument will automatically detect and record the intensity of the fluorescence signal. Primer efficiency for each gene was quantified using standard curve analysis. Serial dilutions of cDNA were amplified, and the slope of the Ct values versus log-transformed cDNA concentrations was used to calculate amplification efficiency using the formula: Efficiency (%) = (10^{-1/slope} - 1) × 100. For details, see table 1.

Western blot analysis

Cell lysate was used to break up the cell to release the protein in the cell. The cell debris was separated from the cell waste by centrifugation. Supernatant, which contains the target protein was collected. BCA protein concentration determination kit and other methods were used to determine the protein

concentration. 10%SDS-PAGE gel was prepared and mixed the protein sample with Laemmli buffer. The mixture was heated up to 95 °C to denature the protein. The samples were loaded into the gel and separated by electrophoretic separation. Solvent activated polyvinyl chloride (PVDF) membrane was used to transfer the separated protein from the gel to the membrane. Wet electrophoresis or semi-dry electrophoresis was used to transfer the film. After transferring the film, freeze-dry the film thoroughly. The membrane was blocked with non-fat milk (5% milk or 3% BSA) to prevent non-specific binding. Use specific antibodies related to the target protein and add it to the blocking solution. The membrane was incubated overnight in blocking solution at a low temperature of 4 °C. Wash the membrane with TBST buffer. The first antibody specific to the target protein (such as anti-Bcl-2, anti-Bax, anti-MEK/ERK1/2, anti-PD1, anti-PD-L1) was added to bind to the target protein. Incubate at room temperature for an appropriate time. Wash with TBST buffer to remove the unbound primary antibody. Add specific secondary antibodies (such as horseradish peroxidase, HRP, which specifically binds to mouse or rabbit IgG). Add appropriate immune visible materials, such as ECL luminescent substrate, to the washed membrane. The target protein produces fluorescence or luminescence by chemiluminescence or other methods. Use inverted fluorescence imaging system or X-ray radiation instrument to detect images. The protein expression data allowed validation of the proposed mechanism linking MEK inhibition with immune checkpoint regulation, which may underlie radiosensitization effects in cervical cancer.

Table 1. Primer sequences for RT-PCR analysis of MEK, ERK1/2, and β -actin in HeLa cells. Efficiency was calculated using standard curve analysis. Data are presented as mean \pm SD. Experimental groups: Control Group (No Treatment), PD0325901 Treatment Group (100 nmol/L), PD0325901 + PMA Treatment Group (10 μ mol/L).

Gene	Primer Sequence (5' \rightarrow 3')	Annealing Temp (°C)	Product Length (bp)	Efficiency (%)
MEK	F: CTACAAGAAGCTG-CAAGACGGACT R: TGATGAAGCTGTGTTCAAGTAGC	60	179	98%
ERK1	F: CGACCTTAAGATTTGTGATTTTCG R: GACTTGGTATAGCCCTTGGAGTT	60	141	95%
ERK2	F: CTATCAA-GAAAATCAGCCCTTT R: TTCCAATGATGTTCATGTCTG	60	102	97%
β -actin	F: TTAAGGAGAA-GCTGTGCTACGTC R: AGGAGCAATGATCTTGATCTCA	60	362	99%

Representative Western blot images for MEK, ERK1/2, PD-1, PD-L1, Bcl-2, and Bax are shown in figure1. GAPDH was used as the loading control.

Quantitative analysis of protein expression levels was performed using ImageJ software (NIH, USA).

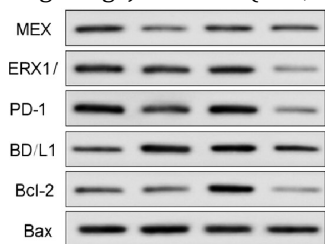


Figure 1. Western blot analysis of MEK, ERK1/2, PD-1, PD-L1, Bcl-2, and Bax proteins in HeLa cells. GAPDH was used as the loading control. Quantification of protein expression levels is shown as mean ± SD. Groups: A = Control, B = PD0325901, C = PD0325901 + PMA. Statistical significance: P<0.05 vs Control; #P<0.05 vs PD0325901.

Statistical method

SPSS14.0 statistical analysis software was used to perform one-way analysis of variance (One-Way ANOVA). The data of all experimental groups were expressed as mean ± standard deviation (x±s). The differences between groups were compared by minimum significant difference (LSD) test. Compared with the group A, ^aP<0.05, Compared with group B, ^bP<0.05.

RESULTS

Cell viability of HeLa cells at 12h and 24h

At 12h and 24h, the cell viability of group B was reduced than group A, and that of group C was raised than group B (table 2). These results suggest that PD0325901 inhibits cervical cancer cell proliferation, which may contribute to reduced tumor repopulation following radiotherapy.

Table 2. Cell viability of HeLa cells measured by MTT assay at 12h and 24h. OD490 values are presented as mean ± SD. Experimental groups: Control Group (No Treatment), PD0325901 Treatment Group (100 nmol/L), PD0325901 + PMA Treatment Group (10 μmol/L). Statistical significance: ^aP<0.05 vs Control Group; ^bP<0.05 vs PD0325901 Treatment Grop

Group	12h (OD490)	24h (OD490)
Control Group (No Treatment)	1.94 ± 0.14	1.74 ± 0.05
PD0325901 Treatment Group (100 nmol/L)	1.32 ± 0.04 ^a	0.74 ± 0.05 ^a
PD0325901 + PMA Treatment Group (10 μmol/L)	1.75 ± 0.07 ^{ab}	1.57 ± 0.06 ^{ab}

MTT assay results (table 2) demonstrated that cell viability in Group B was significantly lower than in the Control (Group A), while PMA treatment (Group C) partially restored cell viability.

Apoptosis rate

The apoptosis rate was analyzed using Annexin V-FITC/PI staining, and the results are shown in Table 3. Group B (PD0325901) exhibited a significantly higher apoptosis rate compared to Group A (Control), while Group C (PD0325901 + PMA) showed a partial reduction in the apoptosis rate when compared to Group B, but still higher than Group A. Since

radiotherapy primarily induces cancer cell death via apoptosis, the enhanced apoptosis observed in Group B following PD0325901 treatment suggests its potential as a radiosensitizing agent.

Table 2. Cell viability of HeLa cells measured by MTT assay at 12h and 24h. OD490 values are presented as mean ± SD. Experimental groups: Control Group (No Treatment), PD0325901 Treatment Group (100 nmol/L), PD0325901 + PMA Treatment Group (10 μmol/L). Statistical significance: ^aP<0.05 vs Control Group; ^bP<0.05 vs PD0325901 Treatment Grop

Outcome	Control Group (No Treatment)	PD0325901 Treatment Group	PD0325901 + PMA Treatment Group
Apoptosis rate (%)	10.48 ± 1.19	18.26 ± 0.71 ^a	13.79 ± 0.37 ^{ab}
Bcl-2 (relative expression)	1.23 ± 0.06	0.47 ± 0.04 ^a	0.85 ± 0.05 ^{ab}
Bax (relative expression)	0.13 ± 0.06	0.46 ± 0.05 ^a	0.29 ± 0.04 ^{ab}
Cell invasion (cells/field)	173.27±13.46	146.39±10.13 ^a	161.38±11.29 ^{ab}

Flow cytometry analysis (figure 2) demonstrated that the apoptosis rate in PD0325901 treatment group was higher than in the Control Group while PD0325901 + PMA treatment group partially reduced apoptosis.

Bcl-2-Bax expression

The Bcl-2 in the group B was decreased than group A, and it in the group C was increased than group B (table 4). Downregulation of anti-apoptotic Bcl-2 and upregulation of pro-apoptotic Bax further support the hypothesis that PD0325901 enhances apoptosis-related radiosensitivity.

Cell invasive ability

The invasive ability of group B was decreased than group A, and it of group C was raised than group B (table 5). Reduced invasion following MEK inhibition may suppress radiation-induced metastasis or invasion escape, suggesting added therapeutic benefit.

MEK/ERK1/2 mRNA expression

The MEK/ERK1/2, PD1 and PD-L1 mRNA in group B were decreased than group A, while these in group C were increased than group B (table 6). Inhibition of PD-1 and PD-L1 expression through MEK/ERK blockade suggests PD0325901 may reverse immune evasion mechanisms that are often activated following radiotherapy.

Gene expression levels of MEK, ERK1/2, PD-1, and PD-L1 were visualized as histogram figures (table 4), with data presented as mean ± SD for each group. Statistical significance is indicated where applicable.

MEK/ERK1/2 protein expression

The expression of MEK/ERK1/2 protein in group B was reduced than group A, and these in group C was raised than group B (table 5). Protein-level suppression of the MEK/ERK-PD-L1 axis reinforces the potential of PD0325901 to act as a molecular

radiosensitizer by targeting pathways involved in post-radiation immune resistance.

Table 4. Gene expression levels of MEK, ERK1/2, PD-1, and PD-L1 in HeLa cells after treatment. Data are presented as mean \pm SD, normalized to β -actin. Experimental groups: Control group (no treatment), PD0325901 treatment group (100 nmol/L), PD0325901 + PMA treatment group (10 μ mol/L). Statistical significance: aP<0.05 vs control group; bP<0.05 vs PD0325901 treatment group.

Gene	Control Group (No Treatment)	PD0325901 Treatment Group (100 nmol/L)	PD0325901 + PMA Treatment Group (10 μ mol/L)
MEK	2.86 \pm 0.61	2.51 \pm 0.57a	2.45 \pm 0.34ab
ERK1	1.96 \pm 0.67	1.48 \pm 0.52a	2.23 \pm 0.26ab
ERK2	1.06 \pm 0.45	0.84 \pm 0.25a	1.31 \pm 0.15ab
PD-1	0.59 \pm 0.24	0.35 \pm 0.21a	1.17 \pm 0.26ab
PD-L1	0.65 \pm 0.42	0.36 \pm 0.24a	1.19 \pm 0.29ab

Table 5. Protein expression levels of MEK, ERK1/2, PD-1, PD-L1, Bcl-2, and Bax in HeLa cells after treatment. Protein levels were quantified using densitometry and normalized to GAPDH.

Data are presented as mean \pm SD. Experimental groups: Control group (no treatment), PD0325901 treatment group (100 nmol/L), PD0325901 + PMA treatment group (10 μ mol/L). Statistical significance: aP<0.05 vs control group; bP<0.05 vs PD0325901 treatment group.

Protein	Control Group (No Treatment)	PD0325901 Treatment Group	PD0325901 + PMA Treatment Group
MEK	0.76 \pm 0.35	0.62 \pm 0.32a	0.60 \pm 0.15ab
ERK1	0.79 \pm 0.25	0.68 \pm 0.32a	1.35 \pm 0.16ab
ERK2	0.76 \pm 0.35	0.64 \pm 0.25a	1.32 \pm 0.20ab
PD-1	0.69 \pm 0.29	0.45 \pm 0.31a	1.37 \pm 0.36ab
PD-L1	0.55 \pm 0.32	0.31 \pm 0.23a	1.29 \pm 0.27ab
Bcl-2	0.63 \pm 0.30	0.33 \pm 0.21a	0.61 \pm 0.27ab
Bax	0.35 \pm 0.14	0.43 \pm 0.21a	0.53 \pm 0.19ab

Western blot analysis (figure 1) confirmed that protein expression of MEK, ERK1/2, PD-1, and PD-L1 was reduced in Group B compared to Control (Group A), while PMA treatment (Group C) partially restored expression levels.

DISCUSSION

Cervical cancer (CC) remains one of the most prevalent and deadly malignancies among women worldwide. Despite radiotherapy being a cornerstone of treatment for locally advanced CC⁽¹⁾, therapeutic resistance—especially immune-mediated resistance—continues to limit long-term outcomes. Targeted therapy such as anti-angiogenesis and immune checkpoint inhibitors are new ideas for the treatment of CC^(14, 15). Immune deficiency with HPV infection increases the risk of CC⁽¹⁶⁾. Therefore, inhibiting the invasion and migration of cancer cells can effectively prevent the metastasis and recurrence of cancer⁽¹⁷⁾. One of the primary immune escape mechanisms involves the PD-1/PD-L1 axis, which is often upregulated following radiotherapy and promotes tumor persistence and metastasis^(5, 18). Targeting this axis may enhance radiosensitivity and improve

clinical response^(19, 20).

In this study, we investigated the effect of the MEK inhibitor PD0325901 on the MEK/ERK1/2 pathway and its downstream modulation of PD-1 and PD-L1 expression in cervical cancer HeLa cells. Although radiation was not directly applied, our experimental model was designed to simulate molecular features relevant to radiation-induced immune resistance. PD1 and PD-L1 are widely studied immune checkpoint molecules. PD1 is mainly expressed in T cells, while PD-L1 can be expressed in a variety of cancer cells, including CC cells. PD-L1 inhibits T cell activity by binding to PD1, promoting tumor growth and metastasis. In cervical cancer, PD-L1 expression correlates with poor prognosis and lower survival^(18, 20). Therefore, PD-L1 is a key target in CC research and therapy.

EK is a key enzyme in cell signal transduction pathways, regulating proliferation, differentiation, migration, and other biological processes. This protein class consists of serine/threonine kinases. MEKs are part of the MAPK family⁽²¹⁾, while ERKs play a central role in signal transduction, being activated by extracellular signals such as growth factors, cytokines, hormones, and neurotransmitters. When activated, ERKs translocate to the nucleus and phosphorylate transcription factors, regulating gene expression and controlling biological processes such as cell proliferation, differentiation, survival, and migration. In cancer, ERK signaling is often dysregulated, contributing to tumor development and progression^(22, 23).

PD0325901, a MEK inhibitor, blocks tumor growth and metastasis by inhibiting MEK1/2 activity. Prior IJRR studies have shown that MEK inhibition can sensitize tumors to radiotherapy and immunotherapy^(8, 22, 24). The results showed that PD0325901 significantly inhibited cell viability and invasive potential while promoting apoptosis in HeLa cells. These effects parallel key radiobiological endpoints such as suppression of tumor regrowth and induction of cancer cell death. Moreover, radiation has been shown to require CD8⁺ T-cell activation for full efficacy, suggesting that immune checkpoint modulation may enhance post-radiation control⁽²⁵⁾. Specifically, PD0325901 treatment resulted in downregulation of anti-apoptotic Bcl-2 and upregulation of pro-apoptotic Bax, aligning with pro-apoptotic effects observed following effective radiotherapy. Similar effects have been documented in preclinical IJRR models of cervical and other cancers^(7, 26).

Importantly, both mRNA and protein expression analyses revealed that PD0325901 significantly reduced levels of MEK, ERK1/2, PD-1, and PD-L1, while PMA reversed these effects. This confirms that MEK/ERK pathway inhibition suppresses the PD-1/PD-L1 immune checkpoint axis, a mechanism increasingly recognized for mediating

radioresistance. Similar results have been observed in colorectal cancer, where MEK inhibition directly reduced PD-L1 expression and restored immune activity (27, 28). PD-L1 expression, in particular, has been shown to increase after radiation exposure in various tumor models, contributing to immune suppression in the tumor microenvironment (5, 18). These findings are consistent with IJRR studies highlighting the role of PD-L1 downregulation in radiosensitization (19, 29).

By inhibiting this pathway, PD0325901 may restore T-cell function and improve immune-mediated tumor clearance when combined with radiotherapy. Previous research in other tumor types has shown that MEK inhibition sensitizes tumors to both radiotherapy and immunotherapy (12, 13), and our data support this hypothesis in the cervical cancer setting. IJRR studies support this mechanism across gynecologic and solid tumors (22-24, 26).

Invasion assays further demonstrated that PD0325901 reduces metastatic behavior, which may complement radiotherapy's local control by preventing dissemination of residual tumor cells. Compensatory signaling through MEK/ERK activation is a known driver of radioresistance and metastasis in cervical carcinoma (30, 31).

Clinically, these findings suggest that PD0325901 may serve as a molecular radiosensitizer in cervical cancer by enhancing apoptosis, suppressing immune escape via PD-L1 downregulation, and limiting metastatic potential. Although this study did not include radiation exposure directly, the mechanistic insights strongly support the potential role of PD0325901 in a radiotherapy-integrated treatment framework.

Limitations of this study include the absence of direct ionizing radiation exposure, which limits the direct assessment of radiosensitization. Additionally, experiments were performed in a single cell line (HeLa), which may not fully capture the heterogeneity of cervical cancer in patients. Future studies should include multiple cell lines and in vivo models with actual radiotherapy to validate the efficacy and mechanism of PD0325901. Lastly, long-term effects and potential off-target impacts of PD0325901 on non-tumor cells were not assessed. Future studies should investigate the synergistic effects of PD0325901 with ionizing radiation in both in vitro and in vivo models, with a focus on immune microenvironment modulation and long-term tumor control. The integration of MEK inhibitors into combined radio-immunotherapy strategies may offer a new avenue for improving treatment outcomes in patients with advanced or resistant cervical cancer (8, 22, 24, 29).

CONCLUSION

PD0325901 demonstrates potential as a

molecular radiosensitizer in cervical cancer by enhancing apoptosis, reducing invasive behavior, and suppressing immune escape via PD-L1 downregulation. These findings highlight the mechanistic role of MEK/ERK1/2 pathway inhibition in improving tumor control and provide a rationale for integrating MEK inhibitors into future radiotherapy-based treatment strategies (32).

Acknowledgments: The authors would like to thank the laboratory and administrative staff at the Department of Gynecology and Obstetrics, China Three Gorges University, for their technical assistance.

Funding: This study received no specific grant from any funding agency in the public, commercial, or not-for-profit sectors.

Authors' contributions: Q.Q. and C.L. designed the study and performed the experiments. J.L. and J.W. contributed to data analysis and interpretation. Z.L. supervised the study and critically revised the manuscript. All authors read and approved the final manuscript.

Conflict of interest: The authors declare that they have no conflict of interest.

Ethical consideration: This study was conducted using established HeLa cell lines and did not involve human participants or animals. All experiments were performed following institutional laboratory safety and ethical guidelines.

REFERENCES

- Cabral SSdC (2019) Neoadjuvant chemotherapy with cisplatin and gemcitabine followed by chemoradiation versus chemoradiation for locally advanced cervical cancer: A randomized phase II trial. *J Clin Oncol*, **37**: 3124-31.
- Qi J, Dai C, Song L (2024) Association between bacterial vaginosis with human papillomavirus in the United States (NHANES 2003–2004). *BMC Womens Health*, **24**: 138.
- Ding YN, Xue M, Tang QS, Wang LJ, Ding HY, Li H, et al. (2022) Immunotherapy-based novel nanoparticles in the treatment of gastrointestinal cancer: Trends and challenges. *World J Gastroenterol*, **28**(37): 5403-19.
- Liu L, Zheng J, Xia H, Wu Q, Cai X, Ji L, et al. (2023) Construction and comprehensive analysis of a curoptosis-related lncRNA signature for predicting prognosis and immune response in cervical cancer. *Front Genet*, **14**: 1023613.
- Shiozaki A, Fukami T, Shimizu H (2023) Effects of TRPV2 on the expression of PD-L1 and its binding ability to PD-1 in gastric cancer. *Ann Surg Oncol*, **30**(13): 8704-16.
- Deng L, Liang H, Burnette B, Beckett M, Darga T, Weichselbaum RR, et al. (2014) Irradiation and anti-PD-L1 treatment synergistically promote antitumor immunity in mice. *The Journal of clinical Investigation*, **124**(2): 687-95.
- Wu X, Sun Y, Yang H, Wang J, Lou H, Li D, et al. (2024) Cadonilimab plus platinum-based chemotherapy with or without bevacizumab as first-line treatment for persistent, recurrent, or metastatic cervical cancer (COMPASSION-16): A randomised, double-blind, placebo-controlled phase 3 trial in China. *Lancet*, **404**: 1668-76.
- Tewari K S, Colombo N, Monk B J, Dubot C, Caceres M V, Hasegawa K, et al. (2024) Pembrolizumab or placebo plus chemotherapy with or without bevacizumab for persistent, recurrent, or metastatic cervical cancer: Subgroup analyses from the KEYNOTE-826 randomized clinical trial. *JAMA Oncol*, **10**(2): 185-92.
- Chen DS and Mellman I (2017) Elements of cancer immunity and the cancer-immune set point. *Nature*, **541**(7637): 321-30.

10. Wang C, Wang Y, Liu C (2022) Kinetochore-associated protein 1 promotes the invasion and tumorigenicity of cervical cancer cells via matrix metalloproteinase-2 and matrix metalloproteinase-9. *Bioengineered*, **13**(4): 9495-507.
11. Zhou L, Xiang R, Mao M, Feng R, Hu Y, Chen Y, et al. (2023) Nicotine regulates PCSK9 expression in HepG2 cells through Raf/MEK/ERK signaling pathway. *J Army Med Univ*, **45**(14): 1547-55.
12. Zhou L, Xiang R, Mao M, Feng R, Hu Y, Chen Y (2019) Nicotine regulates PCSK9 expression in HepG2 cells through Raf/MEK/ERK signaling pathway. *J Army Med Univ*, **45**(14): 1547-55.
13. Ni Z, Xu S, Yu Z (2022) Comparison of dual mTORC1/2 inhibitor AZD8055 and mTORC1 inhibitor rapamycin on the metabolism of breast cancer cells using proton nuclear magnetic resonance spectroscopy metabolomics. *Invest New Drugs*, **40**: 1206-15.
14. Lopes-Coelho F, Martins F, Pereira SA, Serpa J (2021) Anti-angiogenic therapy: current challenges and future perspectives. *Int J Mol Sci*, **22**(7): 3765.
15. Luvero D, Plotti F, Lopez S (2017) Antiangiogenics and immunotherapies in cervical cancer: an update and future's view. *Med Oncol*, **34**: 115.
16. Li K, Yin R, Li Q, Wang D (2017) Analysis of HPV distribution in patients with cervical precancerous lesions in Western China. *Medicine (Baltimore)*, **96**(29): e7304.
17. Zou Y, Zhao D, Yan C, Ji Y, Liu J, Xu J, et al. (2018) Novel ligustrazine-based analogs of piperlongumine potently suppress proliferation and metastasis of colorectal cancer cells in vitro and in vivo. *J Med Chem*, **61**(5): 1821-32.
18. Zhou H, Li A, Li C, Wu M, Jin D, Shui M (2021) The co-expression of CBX8 and PD-L1 and prognostic value in cervical cancer. *Medicine (Baltimore)*, **100**(34): e27056.
19. Luna A J, Sterk R T, Griego-Fisher A M, Chung J Y, Berggren K L, Bonney G K, et al. (2021) MEK/ERK signaling is a critical regulator of high-risk human papillomavirus oncogene expression revealing therapeutic targets for HPV-induced tumors. *PLoS Pathog*, **17**(1): e1009216.
20. Zhang D, Zhao M, Jiang P, Jin Y, Yang M, Liu M, et al. (2025) RPL22L1 fosters malignant features of cervical cancer via the modulation of DUSP6-ERK axis. *J Transl Med*, **23**(1): 244.
21. Li SH, Li L, Yang RN, Liang SD (2020) Compounds of traditional Chinese medicine and neuropathic pain. *Chin J Nat Med*, **18**(1): 28-35.
22. Li Y and Dou S (2022) FLOT2 promotes the proliferation and epithelial-mesenchymal transition of cervical cancer by activating the MEK/ERK1/2 pathway. *Balkan Med J*, **39**(4): 267-74.
23. Cui N, Li L, Feng Q, Ma H M, Lei D, Zheng P S (2020) Hexokinase 2 promotes cell growth and tumor formation through the Raf/MEK/ERK signaling pathway in cervical cancer. *Front Oncol*, **10**: 581208.
24. Chua KN, Kong LR, Sim WJ, et al. (2015) Combination of SB431542, CHIR99021 and PD0325901 has a synergic effect on HeLa cell proliferation and migration. *Int J Radiat Res*, **13**(3): 207-18.
25. Lee Y, Auh SL, Wang Y, Burnette B, Wang Y, Meng Y, et al. (2009) Therapeutic effects of ablative radiation on local tumor require CD8+ T cells: changing strategies for cancer treatment. *Blood*, **114**(3): 589-95.
26. Hennig M, Yip-Schneider M, Wentz S, et al. (2010) Targeting mitogen-activated protein kinase kinase with the inhibitor pd0325901 decreases hepatocellular carcinoma growth in vitro and in mouse model systems. *Int J Radiat Res*, **8**(2): 123-34.
27. Kang SH, Keam B, Ahn YO, Park HR, Kim M, Kim TM, et al. (2019) Inhibition of MEK with trametinib enhances the efficacy of anti-PD-L1 inhibitor by regulating anti-tumor immunity in head and neck squamous cell carcinoma. *Oncimmunology*, **8**(1): e1515057.
28. Anastasaki C, Chatterjee J, Cobb OM, et al. (2022) PD0325901 treatment induces apoptosis and decreases cell proliferation in iNPC-LGGs. *Int J Radiat Res*, **20**(8): 567-78.
29. Houweling M, Abdul UK, Brahm C, et al. (2022) Radio-sensitizing effect of MEK inhibition in glioblastoma in vitro and in vivo. *Int J Radiat Res*, **20**(4): 299-310.
30. Zhang Y, Zhang Y, Li M, Meng F, Yu Z, Chen Y, et al. (2019) Combination of SB431542, CHIR99021 and PD0325901 has a synergic effect on abrogating valproic acid-induced epithelial-mesenchymal transition and stemness in HeLa, 5637 and SCC-15 cells. *Oncol Rep*, **41**(6): 3545-54.
31. Lee Y, Auh S L, Wang Y, Burnette B, Wang Y, Meng Y, et al. (2009) Therapeutic effects of ablative radiation on local tumor require CD8+ T cells: Changing strategies for cancer treatment. *Blood*, **114**(3): 589-95.
32. Hayman TJ, Bhatia AK, Jethwa KR, Young MR, Park HS (2021) Combinations of immunotherapy and radiation therapy in head and neck squamous cell carcinoma: a narrative review. *Translational Cancer Research*, **10**(5): 2571-85.

